Escrivà Bou, À.; Lund, J.; Pulido-Velazquez, M.; Hui, R.; Medellín-Azuara, J. (2018). Developing a water-energy-GHG emissions modeling framework: Insights from an application to California's water system. Environmental Modelling & Software. 109:54-65. doi:10.1016/j.envsoft.2018.07.011

Developing a Water-Energy-GHG Emissions Modeling Framework: Insights from an Application to California's Water System

Alvar Escriva-Bou[1,], Jay R. Lund[2], Manuel Pulido-Velazquez[3] Rui Hui[2], and Josué Medellín-Azuara[2]*

1. Water Policy Center, Public Policy Institute of California. 500 Washington Street, Suite 600. San Francisco, 94111 California. USA.

2. Center for Watershed Sciences, University of California, Davis. One Shields Avenue, Davis, CA. 95616, USA.

3. Research Institute of Water and Environmental Engineering, IIAMA, Universitat Politècnica de València. Camí de Vera S/N, 46022 València, Spain.

Highlights

- We develop an integrated water-energy-GHG emissions model
- Water-related energy use and/or production are included for each water demand
- Water allocation is modeled using a mixed simulation/optimization algorithm
- 13% of electricity and 5% of GHG emissions are related with water use in California
- Several scenarios show the tradeoffs between water, energy, and GHG emissions

Abstract

Integrating processes of water and energy interdependence in water systems can improve the understanding of the tradeoffs between water and energy in management and policy. This study presents a development of an integrated water resources management model that includes water-related energy use and GHG emissions. We apply the model to a simplified representation of California's water system. Accounting for water demands from cities, agriculture, environment and the energy sector, and combining a surface water management model with a simple groundwater model, the model optimizes water use across sectors during shortages from an economic perspective, calculating the associated energy use and electricity generation for each water demand. The results of California's water system show that urban end-uses account for most GHG emissions of the entire water cycle, but large water conveyance produces significant peaks over the summer season. Different policy scenarios show the significant tradeoffs between water, energy, and GHG emissions.

Keywords

Water-Energy Nexus; GHG Emissions; Integrated Water Management; Hydroeconomic Modeling.

Software and/or data availability section

The inputs and outputs are managed via an Excel spreadsheet and the model is programed using Visual Basic for Applications (VBA) and embedded in the spreadsheet. This software can be provided upon request.

All datasets have been obtained from public available sources or from the literature. All the sources and references are included in Section *3.2 Data*.

1. Introduction

A world with more population—rising urban water use, and greater water demands for food and energy production—, a changing climate, and the many water-dependent ecosystems in crisis, challenge how we plan and manage water (Roy *et al.,* 2012; Vörösmarty *et al.,* 2000). At the same time, the high energy use in supplying, conveying, treating and using water, place water systems both as a source of greenhouse gas emissions (Reffold *et al.,* 2008) and as a vulnerable stakeholder facing climate change (Pathak *et* al., 2018; Escriva-Bou *et al.,* 2017). To deal with such complex systems, planners and managers need comprehensive and integrated tools to understand the tradeoffs that involve their decisions.

Although water and energy systems are intricately connected (Gleick, 1994), their analyses have been traditionally studied as separate resources with different approaches. Only during this century, water and energy managers, and researchers have started to look at their interactions. As we show below, recent literature on the water and energy interrelationship can be divided into: a) energy use of water end-uses; b) energy use of water supply, conveyance, treatment and distribution, and wastewater collection, treatment and discharge; and c) water-dependent energy source extraction and electricity generation.

End-uses of water include residential, commercial, industrial and agricultural water uses. The direct energy associated with these water end-uses (without accounting for the embedded energy in upstream actions) is managed directly by customers in heating, electric appliances, industrial processes, pressurizing, etc. Although most water-related energy use is from these end-uses of water (Reffold *et al.* 2008), this is often disregarded in the literature, probably because the effects of the water and energy management actions are driven by the final customers. The heterogeneity of these end-uses also makes the assessment difficult. Researches on urban water uses mostly focus on the residential water-energy relationship (Abdallah and Rosenberg, 2014; Escriva-Bou *et al.* 2015a, 2015b; Fidar *et al.* 2010; Kenway *et al.* 2013; Morales *et al.* 2013), leaving a significant gap for commercial, industrial and other urban end-uses. There are fewer references on energy use from agricultural water end-uses, most of them focused on energy use in pumping and pressurized irrigation technologies (e.g., CEC, 2003; Jackson *et al.* 2010; Rodríguez-Díaz et al., 2011; Daccache et al., 2014).

The most studied part of the water-energy relationship is the urban water cycle. Energy use from various water supply options, treatment and distribution operations, and wastewater collection and treatment, varies widely (e.g., CPUC, 2010b; Mo *et al.* 2014; Mo *et al.* 2011; Nair *et al.* 2014; Plappally and Lienhard, 2012; Raluy *et al.* 2004; Spang and Loge, 2015; Stokes and Horvath, 2009). Some studies also analyze the importance of the embodied energy in large conveyance infrastructure (CPUC, 2010a) or the tradeoffs for various large-scale supply options (Munoz *et al.* 2010).

As energy demand grows, water use for energy generation facilities becomes more important, especially in water stressed regions. In the United States, more than half of the water withdrawals are related to thermoelectric power generation (Healy *et al.* 2015), although most of this use is non-consumptive. Water-related use for power generation is highly variable. Some recent studies provide water-intensity data—the water use per unit of energy generated—across power generation facilities (Macknick *et al.* 2012; Mielke *et al.* 2010; Tidwell *et al.* 2012). Concurrent high temperatures and drought conditions will likely increase energy demands for residential use and water demands for energy generation, which worsens the situation with reduced water availability (Scanlon *et al.* 2013). Some studies asses the water use of energy generation using a life-cycle approach—accounting for all the stages of the product's life—highlighting the high water intensity of biofuel generation (de Fraiture *et al.* 2008; Elena and Esther, 2010).

Finally, many recent articles examine water-energy relationships at regional, national, or supra-national scales. They use available data to summarize water-related energy consumption and/or water use of energy generation (CEC, 2005; Hardy *et al.* 2012; Siddiqi and Anadon, 2011; Tidwell *et al.* 2014; USDOE, 2006).

Most studies reviewed use a static assessment of water and water-related energy interrelation, averaging historical series or estimating the values at a time. Although the results have policy and management applications, they offer less insights for managing dynamic water resource systems. The dynamic approach is a key character of planning and managing models, to ease the decision-making process of a complex water resource system by simplifying the many variables, processes, parameters and uncertainties. Examples include AQUATOOL (Andreu *et al.* 1996), WEAP (Yates *et al.* 2005), CALVIN (Draper *et al.* 2003), MODSIM (Labadie, 2005) and MULINO (Giupponi *et al.* 2004). Although some of these models implicitly include energy-related issues—like hydropower demands or energy costs—none of the models in the literature explicitly account for energy use and GHG emissions of water uses.

This paper develops an economic-based model for water resources system planning and management, including water demands, energy use and GHG emissions of water uses, and water-dependent electricity generation. By including explicitly the energy variables in the development, water allocations vary as a function of the energy and GHG parameters. The model is applied to a simplified California intertied water system, obtaining water and water-related energy and GHG emissions under historical data and environmental conditions. We then run simulations of several scenarios to analyze the tradeoffs between different policies—urban conservation, increased environmental flows, and changing irrigation technologies.

2. Model Objectives and Approach

2.1 Objectives

The main objective of the model is to simulate water allocations across various water uses given historic inflows and groundwater sources, accounting for the energy implications of these water management decisions.

By adapting existing models and analyzing their outputs we could be able to obtain how water outputs translate into energy use and GHG emissions. But specifically we want to assess how considering energy and GHG emission costs can affect water allocation modeling. Questions such as how increasing GHG costs affect water allocations, or how significant is the negative feedback of a region that relies in unsustainable groundwater use when accounting for energy and GHG emission costs, cannot be assessed only by analyzing water model outputs. Because of that we decided to build a new model that can explicitly include the energy variables in the allocation rules.

Some of the potential applications of the model are:

- Assess historical energy use and GHG emissions from water use and their variability.
- Identify promising energy and GHG emission reductions from water conservation or management activities.
- Evaluate water and energy tradeoffs from various water supply strategies or different water demand scenarios.
- Investigate sensitivity of the energy sector to water availability and the suitability of high water-dependent energy generating facilities for the system.
- Estimate the economic value of GHG emissions abatement in the water sector.

2.2 Overall Description

The model has two main sub-models: a surface water management model—spatially represented as a flow network—and a groundwater model—spatially represented as a grid of interconnected cells.

Given reservoir storage, monthly inflows in reservoirs, precipitation over the basin, and demands, the surface model simulates water allocations month by month from the reservoirs to the demands through surface diversions using a mixed simulation-optimization algorithm. First, following a simulation process, water is allocated using a seniority-based approach up to their predefined amounts that represent water rights, contracts or entitlements. When the available water meets the demands the allocation process stops. If there is not enough water the model tries to pump extra groundwater, limited to a given maximum pumping capacity. If still there is not enough water, an economic model allocates the water to minimize scarcity costs—or forgone benefits for deliveries below the maximum demand—within each demand. The optimization algorithm includes also energy and GHG emissions costs, highlighting the role of energy in allocation decisions.

When final allocations—of surface and groundwater sources—are decided, water from non-consumptive use is returned to the surface network and the aquifer to be used later. Energy use from end-uses of water and water supply infrastructure, and water-dependent energy generation from power plants is calculated from final water allocations. Figure 1 shows the processes, including main inputs, decision variables, and model outputs, and Figure 2 shows in more detail the model inputs and outputs.

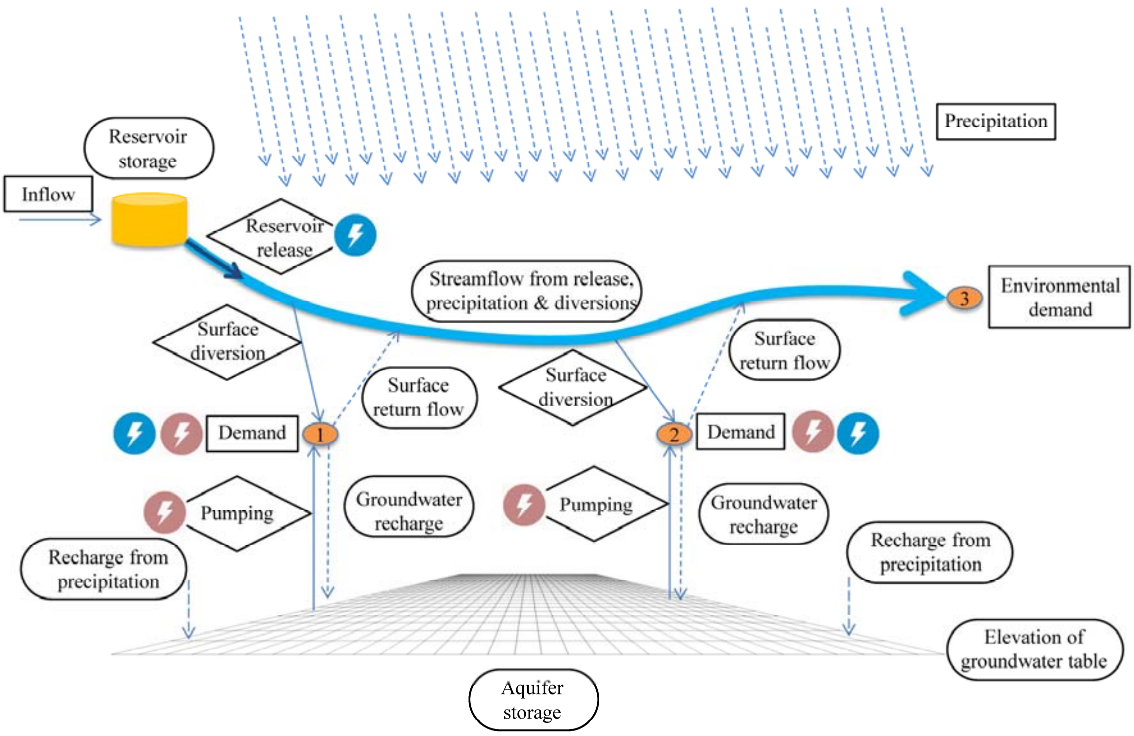

Figure 1: Overview of the processes, variables, and outputs included in the model. Boxes represent input variables, diamonds decision variables, and rounded boxes outputs from the model.

For each month, the model solves a seniority-based simulation algorithm for the releases from reservoirs and an optimization module that minimizes costs (including energy and GHG emission costs) across water users in each node. The model, programmed using Visual Basic for Applications (VBA), is embedded in a Microsoft Excel spreadsheet that includes the input data and also displays the results.

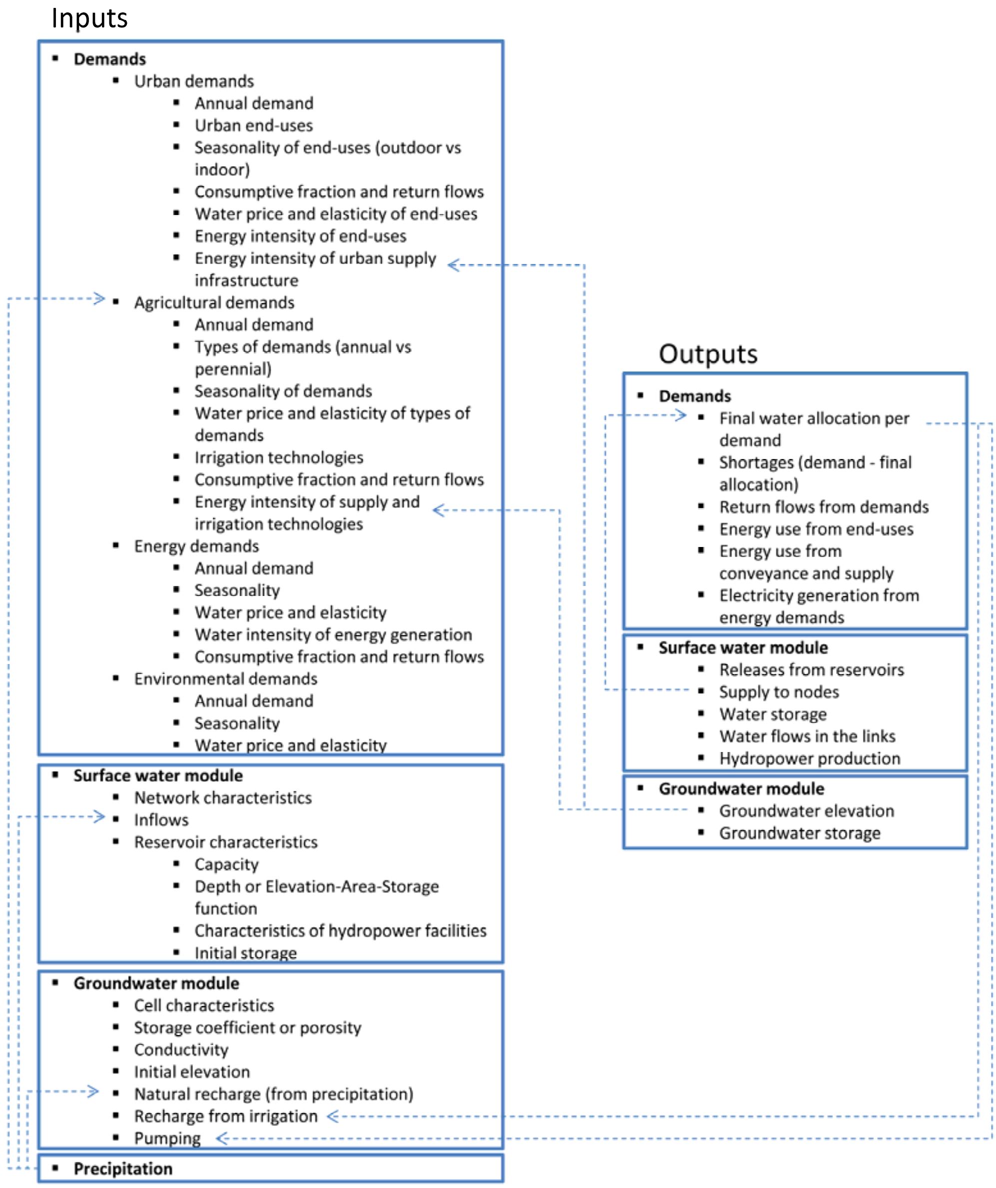

Figure 2: Inputs and outputs of the model, highlighting some of the most important feedbacks of information.

2.3 Methods

2.3.1 Water supply from surface inflow and groundwater

The model represents inflows in two alternative ways. The first is as external surface inflows [Volume · $(\text{Time Step})^{-1}$] to nodes in the surface network. The second is as spatially varying precipitation [Volume · $(\text{Area})^{-1}$ · $(\text{Time Step})^{-1}$] in a cell or cells of the model. The surface inflow can be used at current time step in any demand node, whereas the precipitation becomes runoff in rivers and infiltration into the groundwater storage that will be available in the next time step. Precipitation also affects agricultural demands as explained in more detail below.

The model assumes that 10% of the precipitation goes to the saturated zone of the aquifer in the next time step, 10% goes to streamflow, and the remaining 80% is consumptive use from native vegetation, crops, soil or other land use classes, as a simplification of the Central Valley water data budget from DWR (2014).

2.3.2 Demands

Four main types of demands as input are explained below: urban, agricultural, energy and environmental demands.

2.3.2.1 Urban demands

Urban water demand includes various end-uses by including shares of total consumption: residential single-family, residential multi-family, institutional, commercial, industrial, and landscape irrigation. Each end-use is further divided into outdoor and indoor uses by a parameter. Indoor water use is equally distributed over one year. Monthly outdoor water use varies with precipitation and evapotranspiration. We assume that indoor wastewater returns to a wastewater treatment plant and then back to the surface water network. Outdoor non-consumptive water use returns to the aquifer. From indoor water end-uses and energy-intensity values (CEC, 2005; Escriva-Bou *et al.*, 2015a), we obtain water-related energy use for each water end-use, and further examine if the energy for heating comes from natural gas or electricity with an input parameter.

The energy use of the water utility is quantified by using energy-intensity parameters for water supply, water treatment, water distribution, and wastewater collection and treatment, obtained from CPUC (2010b). Water supply sources include surface water, groundwater, recycled water, brackish desalination, seawater desalination or water transfer. Each source has a maximum supply capacity, a unit cost, a value for its energy intensity, and a priority. Energy intensity of groundwater depends on the groundwater depth obtained from the groundwater model. Water treatment and distribution have different energy intensities depending on the quality of the water source (good, fair or bad) and the geographical characteristics of the city (flat, moderate or hilly). Wastewater collection has an ad-hoc value for its energy intensity whereas wastewater treatment energy intensity depends on treatments levels (primary, secondary and/or tertiary).

From total energy use (end-uses plus urban infrastructure) and fuels used in each stage of the urban water cycle, we estimate GHG emissions by using emission factors. The social cost of CO_2 is obtained using price per ton of emission.

Economic values are also included to obtain scarcity costs of unmet demands. These parameters are the water price and the different price elasticities for each customer category, accounting also for different elasticities for indoor and outdoor uses.

2.3.2.2 Agricultural demands

Agricultural water demands are estimated as a function of the acreage and water requirements by crop in the region. The model considers different irrigation technologies that determine irrigation efficiencies and surface and/or groundwater returns. The model obtains monthly demands from annual demands and monthly evapotranspiration. The monthly demands are also modified if there is precipitation over the region (the monthly precipitation is subtracted to the agricultural monthly demand). After the final allocations are decided and the demand turns into water use, return flows are calculated.

Water-related energy consumption depends on the supply source: surface—with an embedded energy—or groundwater—calculated depending on the groundwater depth. The model also accounts for energy needs of different irrigation technologies. GHG emissions are estimated from energy use similarly as for urban uses.

Water price and water price elasticity are included separately for perennial and annual crops, to calculate scarcity costs for unmet agricultural demands.

2.3.2.3 Energy demands

The water demand of energy generation facilities is obtained by using withdrawal factors—and their consumptive fractions—for electricity generating technologies as a function of the type of generator and its installed capacity using data from Macknick *et al.* (2012) and Mielke *et al.* (2010). Energy generated is calculated from the percentage of working hours per year from CEC (2015). Monthly shares of total annual energy production, monthly freshwater demand and returns are calculated for each facility as input. Hydropower generation is obtained directly from reservoir releases and the power capacity installed in each facility and its efficiency, and the height (more details about the calculation in the Nodes section below).

Similar to urban and agricultural demands, energy demands also have different availability and prices for each source, and water price elasticity is included to quantify costs of potential shortages (Figure 3).

2.3.2.4 Environmental demands

We assume that environmental demand is not necessarily consumptive and it does not use energy. It is only a flow needed at a point or in a stream of the surface network. As inputs, the model needs an annual total demand, monthly shares of this annual demand, and also water price and elasticity for curtailments during shortages.

2.3.3 Surface water management model

The surface water model is represented as a flow network, including 1) nodes with storage (reservoirs) or without storage capacity (junction nodes, diversion nodes) and 2) links (natural streams or artificial channels). The demands are linked to nodes. The network must have an explicit connectivity derived from actual conditions, and a solution algorithm or how to release and allocate water from reservoirs to uses.

2.3.3.1 Nodes

Every node requires conservation of mass. Water entering from the upstream link must be used at the node, stored, or returned to a downstream link or aquifer.

Surface reservoirs are represented by nodes with storage. As inputs, reservoir nodes have maximum capacity, maximum monthly capacity of outlets, and initial storage. A storage-area-elevation curve can be provided, or calculated otherwise. To calculate monthly evaporation and infiltration as a function of current storage, the model also needs average monthly evaporation and seepage rates per area (both in [Volume · Area^{-1} · (Time Step)$^{-1}$]).

If the reservoir has hydropower, the model also needs the water height (obtained from the model using the storage-area-elevation curve), the turbines efficiency, and maximum capacity of the powerhouse to calculate the generated power, as:

$$\boldsymbol{P = \mu \cdot \rho \cdot q \cdot g \cdot h} \quad \text{(Eq. 1)}$$

Where P is available power (W), μ is turbine efficiency, ρ is water density (1000 kg/m^3), q is flow (m^3/s), g is gravity acceleration (m^2/s) and h is available water head (m). In fixed height facilities, the available power is calculated using the minimum from the fixed head and current head values. To obtain energy generation from available power we use the average monthly flow and monthly working hours obtained from this type of facilities in California.

2.3.3.2 Links

Assuming a unidirectional network, every link only connects one node upstream and one downstream (in the flow direction). Although a node can have multiple entering and leaving links, only one link will be the preferred downstream outflow link representing the natural stream that receives return flows. The network connectivity is represented by an *n* x *n* connectivity matrix, where *n* is the number of nodes. The row of the matrix represents upstream nodes and the column represents downstream nodes. This matrix could be a weighted matrix simulating the distance or losses between nodes. For simplicity, only 1 or 0 entries represent connectivity between nodes.

Natural streams are represented as links where water flows downstream. Natural streams have a maximum monthly capacity and seepage rate. The model assumes that rivers can either lose water to the aquifer with a positive infiltration rate, or keep all water with no infiltration. Artificial channels are links where water can either flow downstream or upstream. If it flows upstream, the link will have energy use for pumping.

2.3.3.3 Water allocation algorithm

Monthly allocations are obtained using a mixed simulation/optimization algorithm. First, a priority-based simulation algorithm determines monthly releases from reservoirs to each demand simulating a seniority-based allocation. When total allocation from surface and groundwater sources cannot meet the demands within a node, an optimization module minimizes total scarcity costs allocating water to the highest values, trying to capture a regional reallocation of water. Return flows are obtained from non-consumptive use shares of allocations. The allocations are constrained by reservoir storages, monthly inflows, evaporation and infiltration from reservoirs, returned outflows from demand nodes, and available connectivity from upstream reservoirs. The main steps of the algorithm are described below (and shown graphically in Figure 4).

Step 1: At the beginning of each period, reservoir storages are updated with new inflows.

Step 2: Releases from reservoirs are determined following a seniority-based (priorities) schema:

- Each node can have different types of demand (urban, agricultural, energy generation, and environmental). Each demand has a surface "water right" (the maximum use from reservoirs) and an extra amount that can be met from groundwater (given their pumping capacity, which can be increased by 10% when surface demands are not met with reservoir releases).
- Each surface demand has a priority order, following a prior-appropriation (seniority) based schema. Each node can only get water from its upstream reservoirs or from groundwater.
- Following the priority order, allocations from reservoirs to demands are decided using a simple simulation approach. When there is not enough water to meet all demands, the nodes with lower priorites will face the shortages.
- If all surface demands in a node are met, then groundwater demands are also satisfied, and surface and aquifer return flows are calculated and released.
- If all surface demands of a node are not completely met, the demand tries to pump extra groundwater (up to an extra 50% of its normal groundwater capacity).

Step 3: When all demands in a node cannot be met even with extra groundwater pumping, an optimization model allocates water across different water users (or demands) in a node:

- The optimization module minimizes total scarcity costs (according to water prices and elasticities) plus energy and greenhouse emission costs for all demands at that node. Generally urban outdoor demands are more elastic than indoor demands, annual agricultural crops are more elastic than perennial crops, and energy use is less elastic than anyone else (Figure 3). The minimization problem, which follows a point expansion method (see Griffin, 2016), is:

$$\mathit{Minimize}\ \boldsymbol{Total\,Scarcity\,Cost} = \sum_i \boldsymbol{SC_i} = \sum_i \left[\frac{(\boldsymbol{Q_{0_i}} - \boldsymbol{Q_{s_i}})^2 \cdot \boldsymbol{P_{0_i}}}{2 \cdot |\boldsymbol{\varepsilon_i}| \cdot \boldsymbol{Q_{0_i}}} + \boldsymbol{E_{costs_i}} + \boldsymbol{GHG_{costs_i}}\right] \quad \text{(Eq. 2)}$$

Subject to:

$$\sum_{\mathrm{i}} \left(\mathrm{Q}_{0_\mathrm{i}} - \mathrm{Q}_{\mathrm{s}_\mathrm{i}}\right) = \text{Total Shortage}$$

$$\mathrm{Q}_{0_\mathrm{i}} \geq \mathrm{Q}_{\mathrm{s}_\mathrm{i}}$$

Where *i* is sectorial demand included in the node, $\boldsymbol{SC_i}$ is scarcity cost for demand i, $\boldsymbol{Q_{0_i}}$ and $\boldsymbol{Q_{s_i}}$ are target demand and the actual demand supplied for demand i, $\boldsymbol{P_{0_i}}$ is price of the water for demand i, $\boldsymbol{\varepsilon_i}$ is water price elasticity, E_{costs} are the energy costs, and GHG_{costs} the emission costs for demand *i*.

The solution of this optimization is water supplied for each demand $\boldsymbol{Q_{s_i}}$ and return flows.

Step 4: The releases from each reservoir are the summed releases for each demand at downstream nodes plus spills from reservoir when it achieves the maximum capacity. Reservoir storage for next time step is calculated accounting for evaporation and infiltration, using the average area of the initial and final storage from the elevation-area curve at each time step. Groundwater elevation is also updated given final pumping and groundwater recharge from return flows and precipitation.

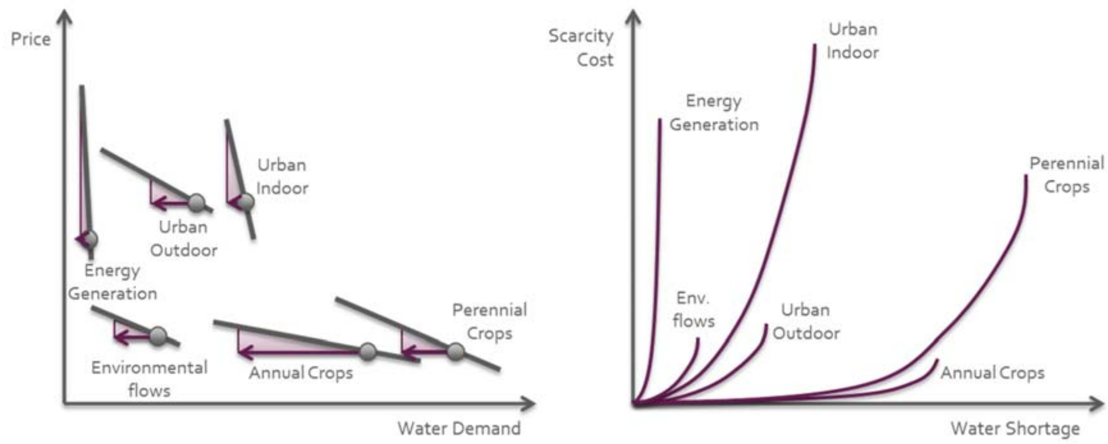

Figure 3: Illustrative water prices and elasticity of water demand, and scarcity cost of water shortage for each water end-uses.

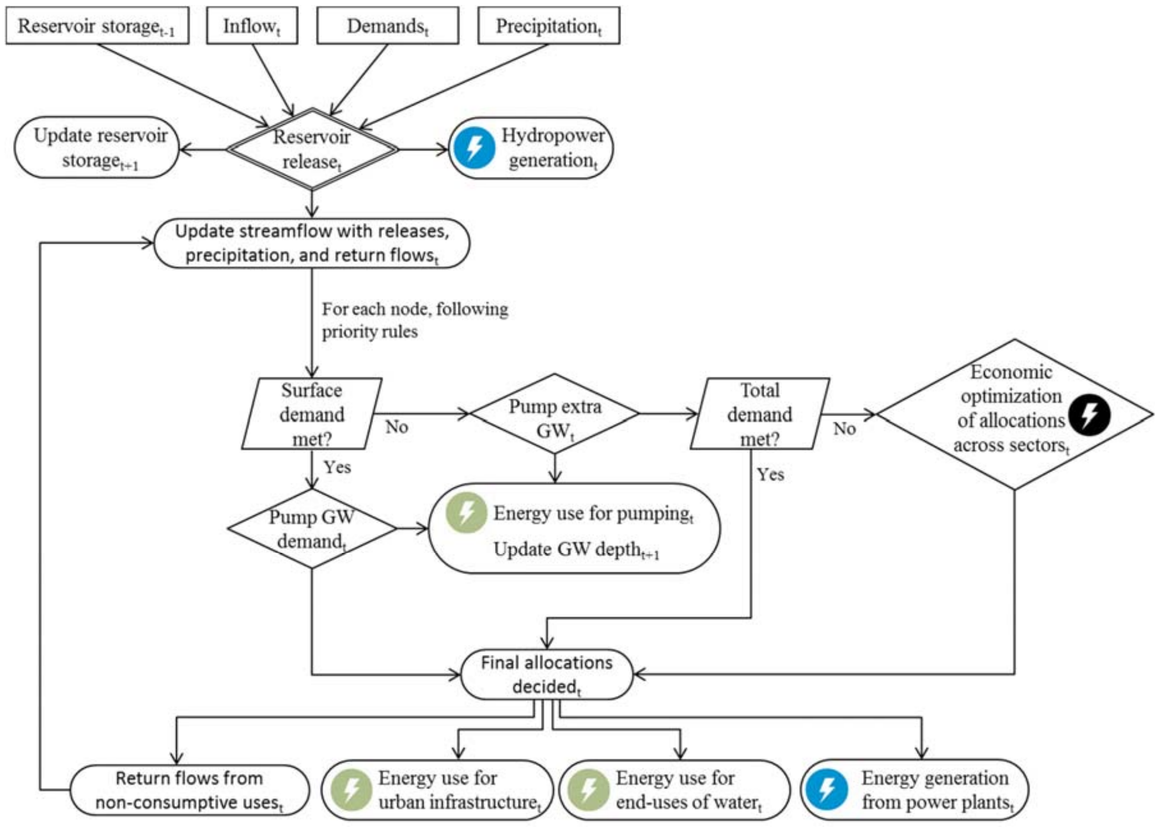

Figure 4: Allocation algorithm used in each time step (monthly in the application shown below). Boxes represent input variables, diamonds decision variables, and rounded boxes outputs from the model. Blue energy icons show energy generation, green energy icons energy use, and black energy icons explicit energy consideration in the optimization algorithm.

2.3.4 Groundwater model

Two options are available to model groundwater: a bucket model and a two-dimensional model. The former form tries to address aquifers that work in isolation from other aquifer interactions, while the latter tries to account for aquifers that can have lateral flows into/from other aquifers or regions.

The bucket model is a simple groundwater reservoir model that has inputs from the percolation of precipitation and recharge from irrigation, and outflows from pumping. At each time step the groundwater depth is calculated as:

$$h_{t+1} = h_t + \frac{(I_t - O_t)}{S \cdot A} \quad \text{(Eq. 3)}$$

Where h is potentiometric head [L]; I_t is inflow and O_t is outflow [L^3]; S is storage coefficient or porosity [dimensionless]; A is area of the cell or bucket [L^2]; and t is time step

A more complex two-dimensional one-layer finite-difference groundwater model simulates non-steady flow for each time step based on a simplification of the MODFLOW model (Harbaugh, 2005). The groundwater flow equation is:

$$\frac{\partial}{\partial x}\left(K_{xx} \cdot \frac{\partial h}{\partial x}\right) + \frac{\partial}{\partial y}\left(K_{yy} \cdot \frac{\partial h}{\partial y}\right) - Q = S_s \cdot \frac{\partial h}{\partial t} \quad \text{(Eq. 4)}$$

where K_{xx} and K_{yy} are the hydraulic conductivities along x and y coordinates [L/T], h is potentiometric head [L], Q is flux per unit of volume that represents sources and/or sinks [1/T], S_s is specific storage [1/L] and t is time step.

Each cell in the bucket model needs only the storage coefficient as a parameter, whereas the two-dimensional model needs horizontal conductivities in each direction and specific storage. Both models need initial groundwater elevation and the sources and/or sinks for each cell and time step. The sources are the precipitation percentage that enters into the aquifer as natural recharge and the return flows from agricultural and urban outdoor uses, and sinks are volumes pumped to meet demands.

2.3.5 Surface and groundwater model integration

Depending on supply source availability, demands can be supplied from surface water and/or groundwater or other available sources. Return flows from non-consumptive use are back to surface water or to aquifer. Reservoirs are connected with aquifers via vertical infiltration rate. Given that pumping is a main drive of energy use and greenhouse gas emissions, the integration of surface and groundwater increases the capability of this model to analyze how demands are met, and takes into account the dynamics of aquifer overdraft.

3. Case study: California intertied water system

3.1 Assembling the model

We applied the developed framework to California's water system, using a simplification that represents the major features of the system. Figure 5 presents a highly simplified schema of California's water resource system for the groundwater and surface water models and corresponding demand and source regions. The grid cells are 100 x 100 km^2 (62.14 x 62.14 $miles^2$), and the green cells have water demands. Each green cell has a population, agricultural acreage and water-dependent energy demand related with a node in the surface water model. Most water use data is at the county level, so we approximate the cell dimensions with the proportion of the California counties included, especially the essential green cells in the model. Table A in the appendix shows how the counties have been assigned to each cell, and how the green cells have an approximated area of 10,000 km^2.

Blue links in the surface network represent natural streams or rivers, whereas red lines represent the major water infrastructures in the California intertied system. C1 is the Friant-Kern Canal; C2-C4 are the California aqueduct; C5 is the San Diego Aqueduct; C6-C8 are the Colorado River Aqueduct, and C9 is the Los Angeles Aqueduct. SR1 to SR9 are nine major reservoirs aggregating main surface storage capacities statewide. Specifically, SR1 to SR9 represent Lake Berryesa, Trinity Lake with Whiskeytown, Shasta, Oroville with Folsom, New Don Pedro with New Melones reservoirs, New Exchequer with Millerton Lake, Pine Flat with Lake Isabella, Haiwe reservoir in the Los Angeles Aqueduct, and Lake Havasu in the Colorado River. Each reservoir receives the aggregated monthly inflow from the more detailed Calvin model (Draper *et al.*, 2003).

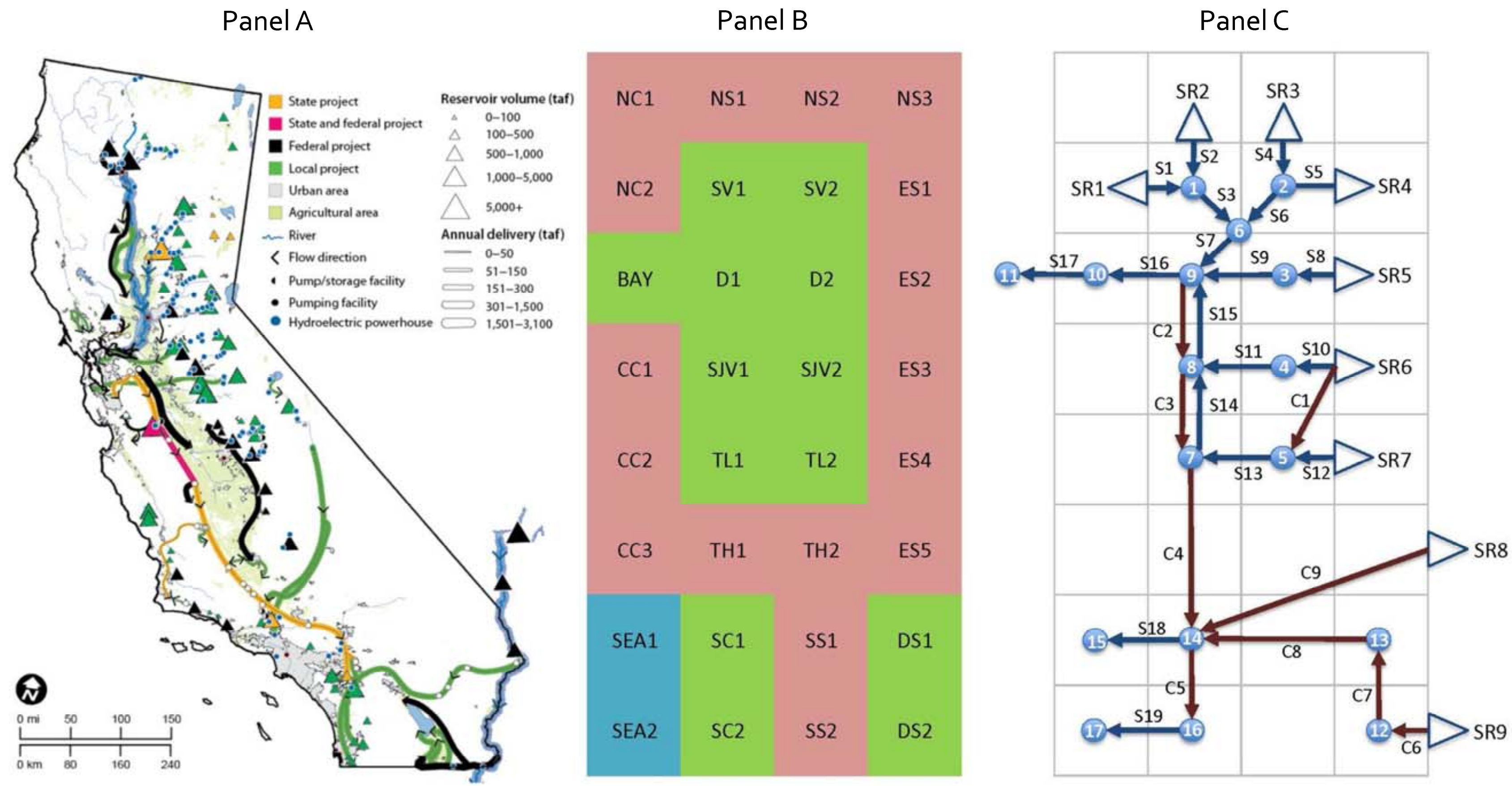

Figure 5: Panel A presents a representation of California water system (from Hanak et al, 2011). Panel B and C present the modeled representation, including respectively the grid cells of the regions, and the corresponding surface water network. [NC: North Coast; NS: Northern Sierra; SV: Sacramento Valley; ES: Eastern Sierra; BAY: Bay Area; D: Delta; CC: Central Coast; SJV: San Joaquin Valley; TL: Tulare; TH: Tehachapi; SEA: (Pacific) Sea; SC: Southern California; SS: Southern Sierra; DS: Desert]

For groundwater we used a mix of the two model options: a bucket model is used for each cell in southern California and the desert regions, and a two-dimensional model is used for the Central Valley (cells SV1, SV2, Bay, D1, D2, SJ1, SJ2, T1 and T2). This tries to represent that whereas the Central Valley has a large interconnected aquifer where lateral flows across regions (represented by cells) is significant, most aquifers in southern California are disconnected from other aquifers, so the interaction is not significant. The rest cells in red are not included in the model and have no interaction with the other cells.

3.2 Data

Annual urban water use by county is from the USGS Water Data (Maupin *et al.*, 2014). From the annual data for 1985, 1990, 1995, 2000 and 2005, we build a monthly data series from October 1984 to September 2003, correcting for seasonality. Agricultural acreage by county is from USDA (2015) and the monthly water necessities are obtained following the method of the California Evapotranspiration Data for Irrigation District Water Balances (ITRC, 2015). Groundwater maximum capacity for urban and agricultural water uses are also from Maupin *et al.* (2014), using the maximum amount that is actually being pumped. Data of energy facilities is from the California Energy Almanac (CEC, 2015), and water consumption per each energy facility is generated using water intensity of energy production (water use per MWh generated) from Macknick *et al.* (2012) and Mielke *et al.* (2010). For environmental flows, we use an annual water demand for node 11 (outflow in the Delta) of 9,900 thousand acre-feet based on average annual delta outflow (DWR, 2015a). Monthly variability is obtained as the average monthly variability of the outflows in the Delta.

Water-related energy use for residential urban end-uses is from Escriva-Bou *et al.* (2015a) and for the other end-uses is from CEC (2005). Energy intensity used in urban, agricultural and energy water supply, treatment, and wastewater collection and treatment is from CPUC (2010b). Water-related energy use for different irrigation technologies is from CEC (2003). Energy intensity of the California Aqueduct and the Colorado River Aqueduct is from Wilkinson (2007).

The groundwater model uses precipitation from Livneh *et al.* (2014), groundwater elevations from DWR (2015b), and aquifer storage coefficients, conductivities, and specific storage from C2VSim (Brush *et al.* 2013). Inflows for the surface model are from the CALVIN model (Draper *et al.* 2003).

3.3 Scenario simulations

We ran several scenarios with the model:

I. Business-As-Usual (BAU): we used the historical 1985-2003 data to run the model. This scenario has an increased urban water demand from roughly 6 to 7.5 MAF, and a decreased agricultural water demand from 40 to 35 MAF. It also considers an implicit increase in more efficient irrigation technologies (from flood irrigation to drip or sprinkle) that decreases irrigation water and recharge but increases energy use. Water-dependent energy facilities are a minor part of California water uses, because the largest thermoelectric energy facilities in California are cooled with seawater.

II. Urban conservation: we simulate a decrease of 20% in total urban use to assess the decreased energy consumption and increased agricultural benefits from reducing shortages.

III. Inefficient irrigation technologies: to analyze the effects of the modernized irrigation technologies, we compare a scenario with a constant share of irrigation technologies as they were in 1985 against a scenario with the development in 2003.

IV. Increased environmental flows: environmental concerns about the Sacramento-San Joaquin Delta health are likely to increase environmental flows. We run a case with increased environmental outflows from the Delta by 50% to assess the effects on the whole system.

V. BAU – No energy and GHG costs: a final scenario compares how water allocations vary when energy and GHG emissions are not included in the optimization (Eq. 2). Note that the optimization module only runs after the seniority base module runs and shortages appear. This scenario might provide some insights of what can traditional models lack when simulating water allocations without accounting for energy and GHG emission costs.

3.4 Results

The model produces a wide range of monthly results. The most significant ones are water allocations (and shortages) per region, storage in surface reservoir and aquifers, energy generation—including hydropower, which is based in reservoir releases, but also from other type of facilities—, water-related energy use, and water-related GHG emissions.

The system is unable to meet the demands during the 1987-1992 drought and, with less importance, during the 2001-03 dry period (Figure 6). The modeled environmental flows, and the Tulare basin, San Joaquin Valley, and Delta demands were severely curtailed. Due to the economic objective that governs allocations, most unmet demands occur in agriculture.

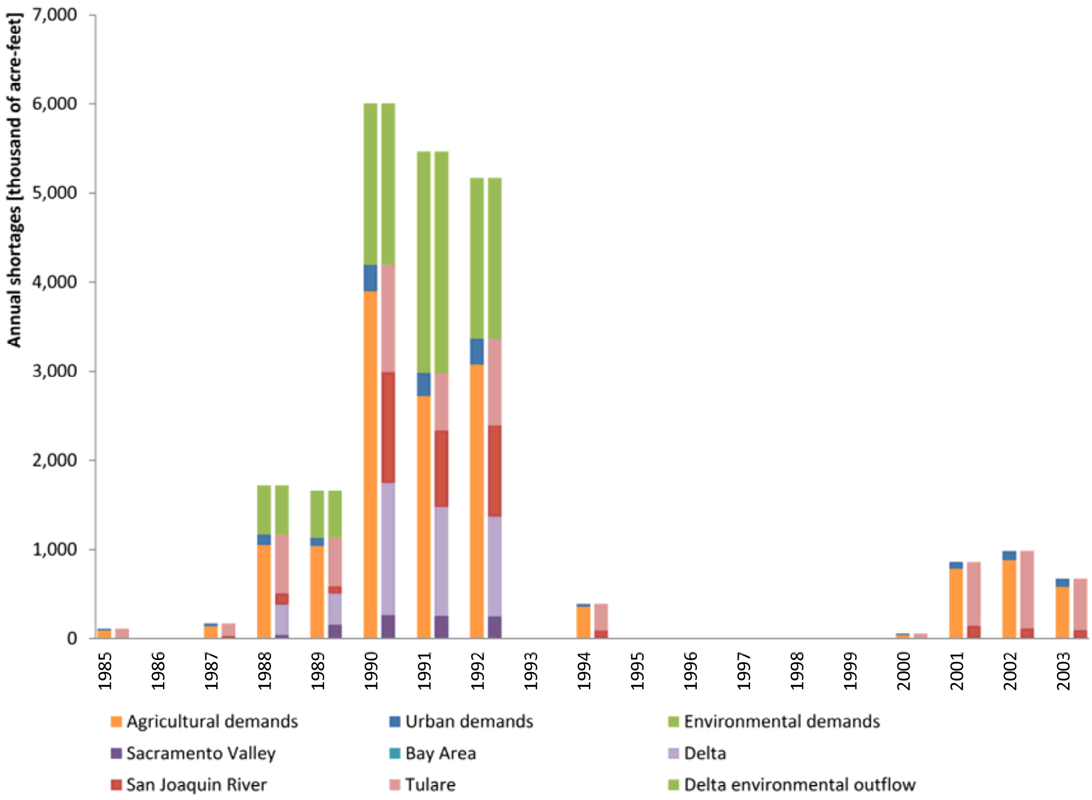

Figure 6: Annual shortages by type of demand (left column) and region (right column)

Figure 7 (top) shows that most water-related energy is urban-related (85.4%), especially from water end-uses (mostly water heating at homes). However, large infrastructure pumping through the California Aqueduct and the Colorado River Aqueduct (11.4%) and agricultural water-related energy (3.2%) are substantial water-related energy uses in California, and coincide with summer energy peaks. Electricity consumption from the entire modeled water cycle is 40,899 GWh/year on average, which is roughly 14% of electricity use in California. Variation of GHG emissions over time and across different uses exhibits similar trend as the water-related energy use in Figure 7 (bottom), as we relate GHG emission directly to energy use. Overall, according to our model, the water cycle emits about 21.5 million tons of CO_2, about 5% of total per capita GHG emissions statewide.

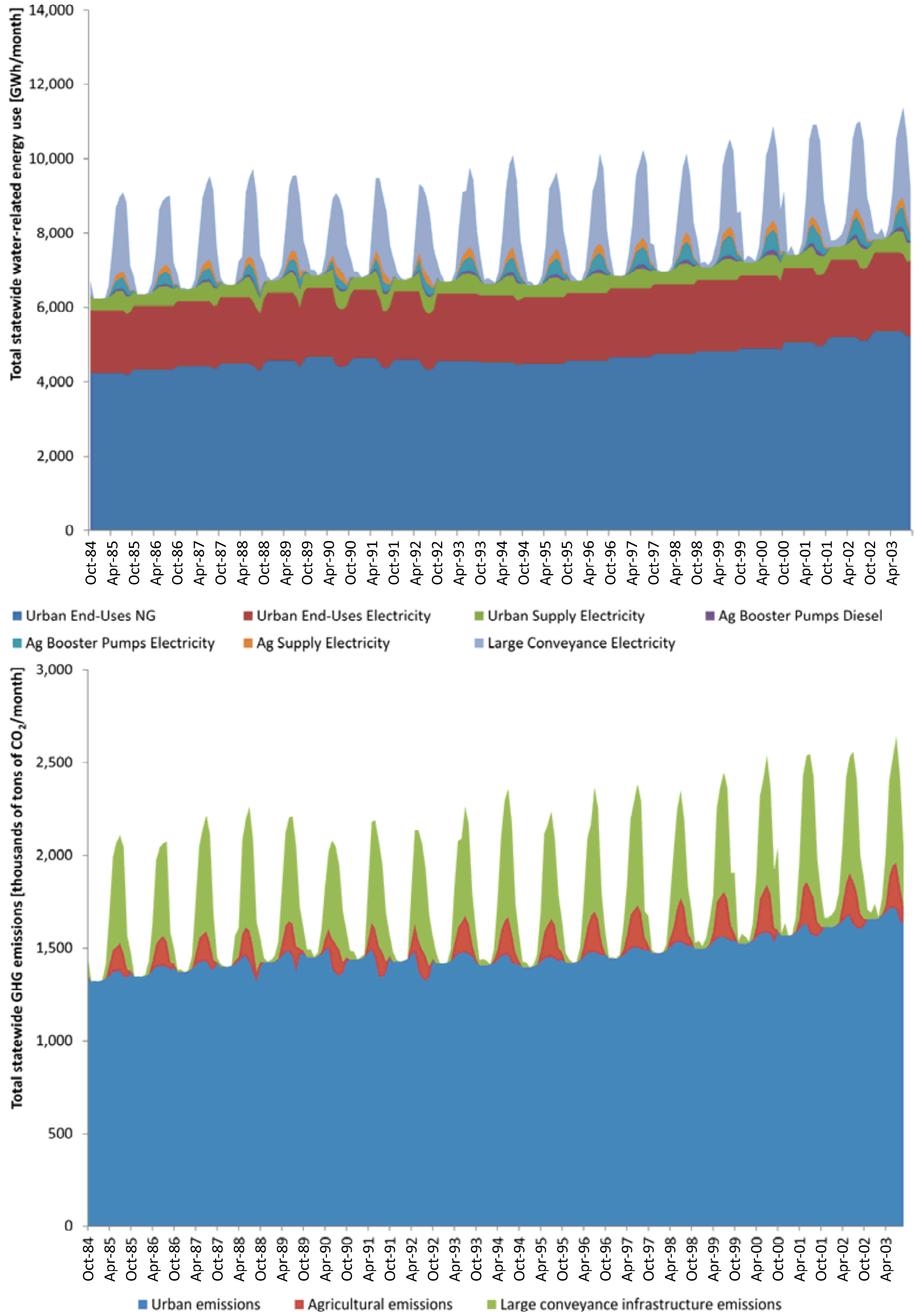

Figure 7: Statewide (top) water-related energy use and (bottom) GHG emission during the modeling period

Energy use, GHG emission, hydropower generation, groundwater overdraft and water supply shortage vary greatly for the different scenarios (Table 1). Compared to the BAU case, urban conservation has a huge potential to save energy and CO_2 emissions and would also reduce groundwater overdraft significantly. Modern irrigation technologies need more energy and have higher irrigation efficiency. Without the irrigation technology development, energy use in agriculture would have been 17% lower but total water shortages 4% higher. Increased environmental flows in the Sacramento-San Joaquin Delta would decrease hydropower generation and cause severe water shortages (although most would be environmental shortages). It also lowers exports from the Delta through the California Aqueduct.

Finally, a run without accounting for energy and GHG emission costs in the allocation algorithm shows similar total shortages but a total different allocation, where urbans are almost never curtailed while agriculture is always worse off. Although these results are totally dependent in our underlying assumptions, the scenario shows the value of accounting for energy and GHG emissions. The system benefits by curtailing a little urban users (mostly from outdoor uses) which have higher energy intensity per unit of water.

Table 1: Comparison of the results for the different scenario runs.

Variable	BAU	Urban conservation		Inefficient irrigation technologies		Environmental flows		BAU No energy & GHG costs	
		Level change	% change	Level change	% change	Level change	% change	Level change	% change
Total water shortages *(taf/year)*	1,224	1,218	-0.5%	1,275	4%	2,910	138%	1,227	0.2%
Agricultural water shortages *(taf/year)*	772	774	0.3%	823	7%	1,312	70%	846	10%
Urban water shortages *(taf/year)*	75	59	-22%	77	3%	117	56%	3	-96%
Environmental water shortages *(taf/year)*	378	384	2%	376	-1%	1,482	292%	377	-0.3%
Total groundwater overdraft *(taf/year)*	3,841	3,358	-13%	3,796	-1%	3,751	-2%	3,873	1%
Hydropower generation *(GWh/year)*	8,622	8,692	1%	8,605	-0.2%	7,438	-14%	8,624	0.0%
Urban end-uses energy use *(GWh/year)*	77,868	62,302	-20%	77,854	0.0%	77,574	-0.4%	78,411	1%
Urban infrastructure energy use *(GWh/year)*	5,117	4,094	-20%	5,115	0.0%	5,085	-1%	5,172	1%
Agricultural energy use *(GWh/year)*	3,122	3,112	-0.3%	2,599	-17%	3,068	-2%	3,117	-0.2%
Large-conveyance energy use *(GWh/year)*	11,101	10,460	-6%	11,107	0.1%	10,862	-2%	11,096	0.0%
Total energy use *(GWh/year)*	97,208	79,968	-18%	96,677	-0.5%	96,590	-1%	97,797	0.6%
Total electricity use *(GWh/year)*	40,899	34,842	-18%	40,471	-0.5%	40,427	-1%	41,232	0.6%
Total natural gas use *(GWh/year)*	55,932	44,749	-18%	55,925	-0.5%	55,791	-1%	56,188	0.6%
Total diesel use *(GWh/year)*	378	378	0%	280	-25.7%	371	-2%	377	-0.3%
GHG emissions *(million tons CO_2/year)*	21.5	17.8	-17%	21.4	-0.5%	21.4	-0.5%	21.7	1%

4. Comparison of the results with other models and actual data

Although the main objective of this paper is not to match the results of the California system, in the following subsections we present some comparison of the model results with actual data or results from other models to analyze our model's ability to represent the system.

4.1 Water shortages

The state, nor any other entity, releases actual data of water shortages at the state level. Other models, like CALVIN (Draper *et al*., 2003), do rely on shortages to obtain the economic costs and optimal allocation of water. Unfortunately we did not find any study that presents annual water shortages. At the aggregated level, Harou *et al.* (2010), using CALVIN, found an average scarcity of 1.6 maf/year for the period 1922-1993, which is 30% higher to our estimate of 1.2 maf/year.

As a proxy for shortages we can use the water deliveries from the Delta through the Central Valley Project and State Water Project. More than 25 million people and about 3 million acres of irrigated lands rely on these exports (Mount *et al*., 2016), and the deliveries vary year to year depending on the water conditions, storage, and environmental regulations. As Figure 8 shows, Delta deliveries vary from 3 maf to over 6 maf, causing actual supply shortages south of the Delta that have to be replaced with stored water or extra groundwater pumping. The figure also shows that our representation of the exports obtained from the model follows similar patterns to what actually happened. Our maximum estimate is larger, and this might be caused because we did not limit the capacity of the infrastructure.

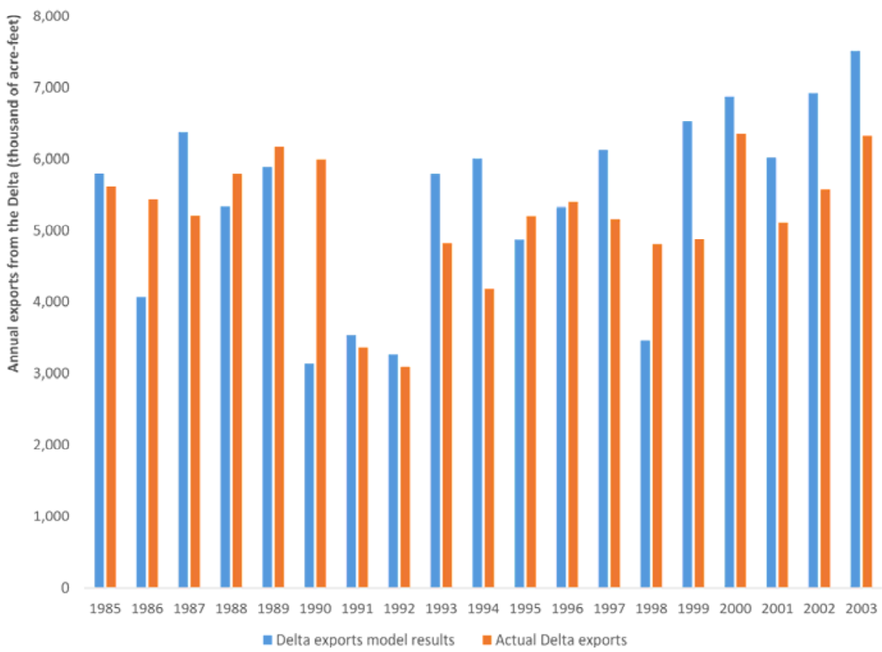

Figure 8: Actual data and model results for the Delta exports.

Howitt *et al.* (2015) analyzed the economic consequences of the 2015 drought for California agriculture. This study can help in assessing the reliability of our results, given that the 2012-16 drought was similar to the 1987-92. Howitt *et al.* (2015) found that the surface water shortage in 2015 was 8.7 maf, but most of this (up to 6 maf) was substituted by groundwater, so the final shortage was of 2.7 maf. Note that they only accounted for agricultural shortages, without including environmental or urban shortages. Looking at the regional effects, the Tulare Basin was hit hardest.

Our results also find that the shortages are always tougher in the Tulare Basin, followed by the San Joaquin and the Delta regions. The largest shortage that we find is 6 maf (for 1990), but 1.8 maf of that is environmental flow shortages in the Delta and almost 300 taf of urban shortages, so the final agricultural shortage is 3.9 maf. That might mean that our model is overestimating a little shortages by not using enough groundwater substitution.

4.2 Groundwater

Changes in groundwater elevation from 1985 to 2003 show that the southern part of the Central Valley and the Southern Coast regions are overdrafting their aquifers. Because of higher precipitation and more surface water availability, groundwater elevation increases in Sacramento Valley and the eastern Delta. The Tulare Basin is the region with more overdraft and depletes the aquifer even in wet years. The total groundwater overdraft for the regions considered would be 73 MAF after the 19 years modeling period and on average over 3.8 MAF/year.

To assess our results we obtain the groundwater budget at the subregional level from the California Central Valley Groundwater-Surface Water Simulation Model - C2VSim (Brush *et al.,* 2013). The comparison of the results (Figure 9) shows that our model represents the general trend, but is unable to capture the annual variability. It looks that our model is not replenishing enough the aquifers during wet years in the southern part of the Valley (especially in the Tulare basin), and also is accumulating water in the Sacramento Valley. This might be caused because we are not modeling the river-aquifer connection: on one hand we do not have recharge from rivers and streams (what can be causing an overestimation of overdraft and the no response during wet years), and on the other hand the aquifer is not discharging in the river (what causes the accumulation in the Sacramento Valley.

It’s worth to mention that the annual overdraft for the Central Valley according to C2VSim is 1.8 maf/year—with over 1.2 maf/year in the Tulare basin—whereas we are obtaining 2.5 maf/year for the whole Central Valley and 1.7 maf/year in the Tulare Basin.

Other models, like CVHM (Faunt *et al.*, 2016) estimate a higher rate of overdraft than C2VSim for the Central Valley.

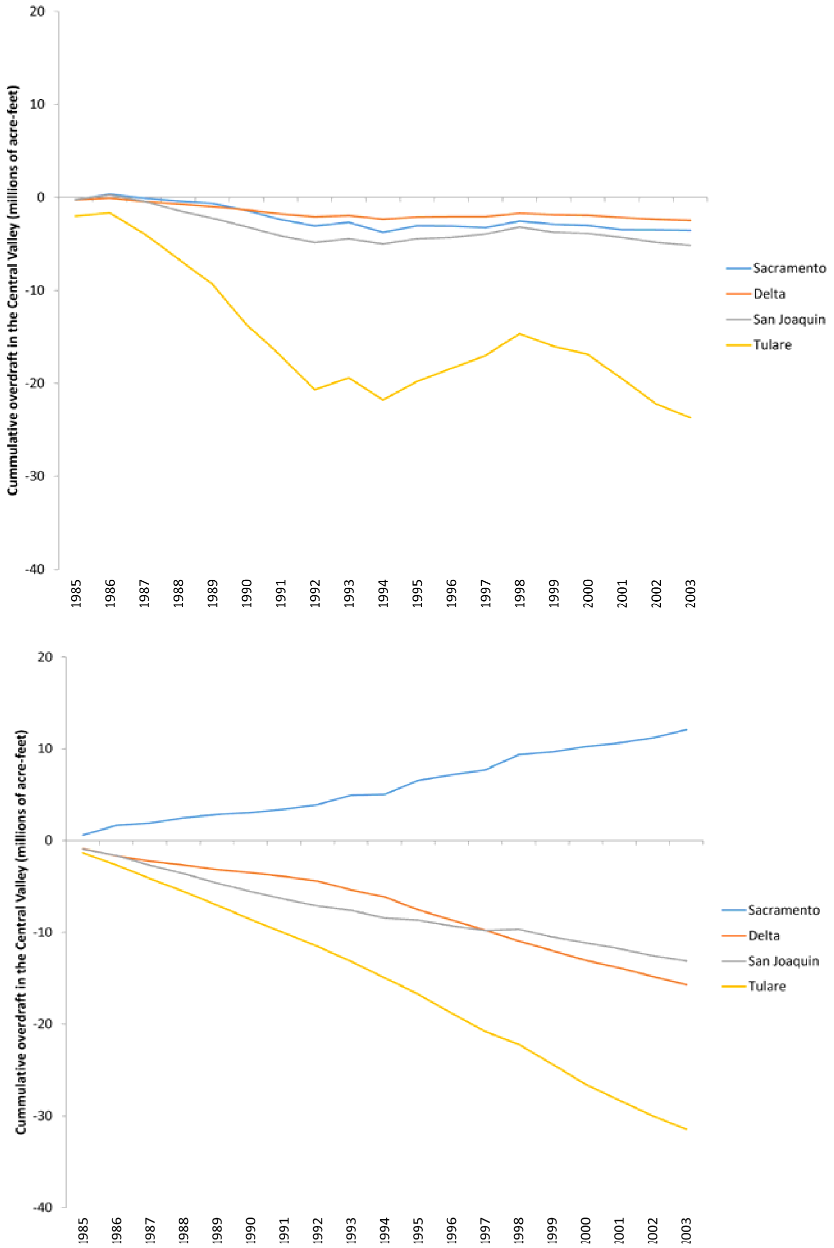

Figure 9: Cummulative aquifer overdraft in the Central Valley at the regional level from C2VSim (top) and from our model (bottom)

4.3 Energy use of the water cycle

In 2005 the California Energy Commission published the first comprehensive assessment of the energy use of the California water system. They estimated that 48,012 GWh every year—19.2% of total electricity use in California—were used in water-related activities. Also 4,284 million therms of natural gas (32% of statewide use). These estimates have been reassessed later (CPUC, 2010a). In CPUC (2010a) the total water sector electricity use (excluding end-uses of water) amounts 18,282 GWh, or 7.7% of statewide electricity use.

Excluding end-uses we obtain 19,340 GWh per year: 5,117 GWh in cities, 3,122 GWh in farms, and 11,101 GWh from large conveyance infrastructure (accounting for the State Water Project and the Colorado River Aqueduct).

When accounting for end-uses, our total estimate for electricity is 40,899 GWh/year, which is 15% lower than the 48,012 GWh estimated by the California Energy Commission for 2001. Two sources of uncertainty may explain these differences: an underestimation of demands and infrastructure in our model, and different methods to estimate energy intensity especially of the end-uses of water.

To add a final point to validate our model it is worth to mention a new study on the effects of water conservation on the energy cycle. In April 2015, the Governor of California mandated a 25% reduction in urban water use relative to 2013 levels. Spang *et al.* (2018) obtained that this policy resulted in 1,830 GWh of electricity savings (note that they only account for water infrastructure energy use, and exclude end-uses of water). For our water conservation scenario (a 20% reduction in urban use) we obtain a reduction of 17,239 GWh of savings when accounting for end-uses of water. But if we only look at the urban supply reduction, including the reduction in energy used in water conveyed to Southern California for urban uses, the reduction on electricity use is 1,663 GWh, which is really close to what Spang *et al.* (2018) obtained.

4.4 Hydropower

Hydropower from reservoir releases presents a similar behavior of California's actual hydropower data obtained from CEC (2015). The model includes only 12 hydropower facilities in California that account for roughly 20% of statewide installed capacity. According to the model results, the total hydropower generated is 18.4% of the actual total generation.

Figure 10 shows the modeled hydropower, the statewide hydropower factored by the share of hydropower capacity included in the model, and then the total statewide hydropower. The results show that during 1990 and 1991 the reservoirs in the model were so empty that hydropower is almost negligible, whereas in the wet period of 1995-2000 the hydropower modeled is much higher than the statewide hydropower for the share of capacity included in the model.

These results make sense if we account that the reservoirs that we included in the model are those in the rim of the Central Valley which are built mainly for water supply purposes. There are many small reservoirs in higher elevations that are built only for electricity generation and even in dry years they produce hydroelectricity by using the scarce passing flows with high heads. It is because of that that the reservoirs that we modeled have higher variability than the statewide actual hydropower production.

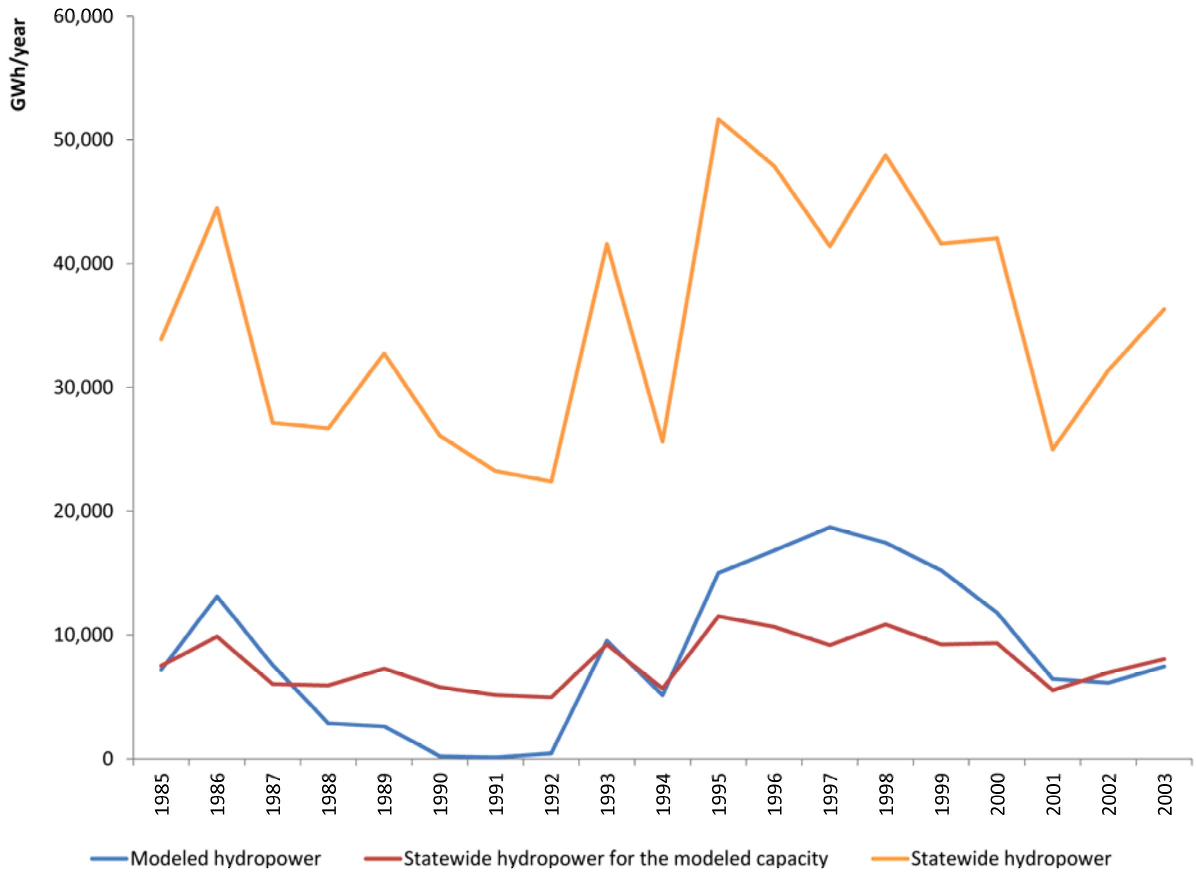

Figure 10: Comparison of modeled hydropower and total hydropower generated in California from CEC (2015)

5. Discussion

We presented an initial development of a water system modeling framework that tries to show the tradeoffs between water, energy and GHG emissions. Most of the inputs are based on literature research—*e.g.* agricultural water necessities, water-related energy intensity for all water uses and processes, water-intensity of energy generation, water prices and elasticities—and the outcomes are sensitivity to them. The outcomes from our simplified model have general implications for decision-making.

The surface and groundwater sub-models need enhancements to present more accurate results. The surface model algorithm could be improved to simulate and optimize the best options for the system beyond releases from reservoirs. The groundwater approach would benefit from a better representation of the river-aquifer interaction and a spatially distributed hydrologic model that could be employed by using different tanks for each model cell for different fluxes (evapotranspiration from crops and native vegetation, infiltration, percolation as vertical fluxes and direct runoff, interflow, base flow and groundwater outflow as horizontal fluxes) and storages (root, non-saturated and aquifer storages) following the methodology of the Sacramento Soil Moisture Accounting (SAC-SMA) model (Sorooshian et al., 1993) or the TETIS model (Frances et al., 2002). An integration of the modeling framework with the Soil and Water Assessment Tool (Arnold *et al*., 1994) could also be possible to face these challenges.

The results of the scenario with no energy and GHG emissions costs shows how allocations across sectors change when energy costs and GHG emission abatement benefits are included. And note that our optimization only works when shortages appear. Therefore, another potential development is to develop an optimization model to analyze the optimal management options that could be taken under different scenarios. The optimization model mentioned above includes economic characteristics in every sub-module, where a hydro-economic optimization for the whole system is desirable. With this development, our model could provide the most economically efficient management options from the different strategies, especially those related with energy savings and GHG emission abatement, to inform policy and decision makers.

Our model also shows which water end-uses are curtailed in a shortage. Most models do not differentiate end-uses within one type of water demand. When a shortage appears, all end-uses are curtailed proportionately in those models. This is not the real performance of a water system.

When water is insufficient for a given demand group (e.g. agriculture, urban), low-valued end water uses are curtailed first, i.e. outdoor uses in an urban demand or low-valued crops in an agricultural demand. This has many implications on the downstream uses. For example, if urban outdoor uses are curtailed first, urban water-related energy, which come mostly with indoor uses, will not be affected until indoor water uses decrease. To account for this behavior, we separate indoor and outdoor uses for all the end-uses in a city, and separate annual and perennial crops in agricultural demands.

6. Conclusions

In this research, a modeling framework has been developed to deal with large-scale water management accounting for water-related energy use and GHG emissions, and water-dependent energy facilities. We obtain that water allocations and shortages change when considering energy and GHG emission costs. Urban water users, much more energy intensive, get curtailed much more with respect to a scenario with no consideration of energy and GHG emission costs.

The model has been applied to the California water system for the 1985-2003 period. Throughout this time period, the California water system could not meet all water demands with frequent shortages. The results from our model show that California's statewide water-related energy use is nearly 100,000 GWh/year, with 85.4% used in cities, 3.2% in agricultural and 11.4% in large-conveyance infrastructures (California aqueduct and Colorado River Aqueduct). Most water-related energy is for heating water in gas-fired water heaters. The electricity use, 40.899 GWh/year, represents 14% of total electricity consumption in California. The carbon footprint of the entire water cycle during the modeling period is 21.5 million tons of CO_2/year, roughly 5% of California's total GHG emissions. These results are lower than other previous estimates because we might be underestimating some of demands and infrastructure in our model, and because of the different methods used to estimate energy intensity especially of the end-uses of water.

The simulations results explicitly show tradeoffs between water and energy in many management options. Improvements in irrigation efficiency save water but have increased energy use in agriculture by 17% in California between 1985 and 2003, so energy-stressed regions might avoid such policies or consider the development of renewable energies associated with them. Increased environmental flows leave less surface water for cities and farms, so they would increase groundwater pumping if allowed by water regulations or transfer energy-intensive water with more energy use. Urban water conservation reduces shortages and aquifer overdraft due to less water pumping. At the same time, it might be a good option to save water-related energy and GHG emissions because urban users are the most energy-intensive water users.

This paper presents a complex water system analysis in a simple excel-based model including also the water, energy, and GHG emissions relations. The results have been also compared with actual data and other models' results. The model shows some agreement with other previous studies but also presents some limitations.

The formulation is applicable to other water and energy systems. As a system of systems concurrently operated, numerous scenarios to provide management options are available by changing characteristic parameters. The development of this research contributes to decision-making in water-energy systems to better inform management, technical and policy discussions.

Funding

This research did not receive any specific grant from funding agencies in the public, commercial, or not-for-profit sectors.

References

Abdallah, A., & Rosenberg, D. (2014). Heterogeneous Residential Water and Energy Linkages and Implications for Conservation and Management. Journal of Water Resources Planning and Management, 140(3), 288-297. doi: doi:10.1061/(ASCE)WR.1943-5452.0000340

Andreu, J., Capilla, J., & Sanchis, E. (1996). AQUATOOL, a generalized decision-support system for water-resources planning and operational management. Journal of Hydrology, 177(3-4), 269-291. doi: Doi 10.1016/0022-1694(95)02963-X

Arnold, B, and Escriva-Bou, A. (2017). Water Stress and a Changing San Joaquin Valley. Technical Appendix A: The San Joaquin Valley's Water Balance. Public Policy Institute of California, San Francisco, CA. Available online at http://www.ppic.org/content/pubs/other/0317EHR_appendix.pdf

Arnold, J. G., Williams, J. R., Srinivasan, R., King, K. W., & Griggs, R. H. (1994). SWAT: Soil and water assessment tool. *US Department of Agriculture, Agricultural Research Service, Grassland, Soil and Water Research Laboratory, Temple, TX*.

Brush, C. F., Dogrul, E. C., & Kadir, T. N. (2013). Development and Calibration of the California Central Valley Groundwater-Surface Water Simulation Model (C2VSim), Version 3.02-CG: DWR Technical Memorandum.

CEC. (2003). California Agricultural Water Electrical Energy Requirements. ITRC Report No. R 03-006. California Energy Commission. Sacramento. December 2003.

CEC. (2005). California's Water - Energy Relationship. Prepared in Support of the 2005 Integrated Energy Policy Report Proceeding. California Energy Commission. November 2005. CEC-700-2005-011-SF.

CEC. (2015). Electric Generation Capacity & Energy. Energy Almanac. California Energy Commission. Online resource available at: http://www.energyalmanac.ca.gov/. Accessed on June 19, 2015.

CPUC. (2010a). Embedded Energy in Water Studies. Study 1: Statewide and Regional Water-Energy Relationship. Prepared by GEI Consultants/Navigant Consulting, Inc. California Public Utilities Commission. August 31, 2010.

CPUC. (2010b). Study 2: Water agency and function component study and embedded energy-water load profiles. San Francisco, CA, USA: California Public Utilities Commission.

Daccache, A., Ciurana1, J.S., Rodriguez Diaz, J.A., Knox, J.W., 2014. Water and energy footprint of irrigated agriculture in the Mediterranean region. Environ. Res. Lett. 9, 1e12

De Fraiture, C., Giordano, M., & Liao, Y. S. (2008). Biofuels and implications for agricultural water use: blue impacts of green energy. Water Policy, 10, 67-81. doi: Doi 10.2166/Wp.2008.054

Draper, A. J., Jenkins, M. W., Kirby, K. W., Lund, J. R., & Howitt, R. E. (2003). Economic-engineering optimization for California water management. Journal of Water Resources Planning and Management-Asce, 129(3), 155-164. doi: Doi 10.1061/(Asce)0733-9496(2003)129:3(155)

DWR. (2014). California Water Plan Update 2013. Department of Water Resources. Online resource available at: http://www.waterplan.water.ca.gov/cwpu2013/final/index.cfm. Accessed July 8, 2015.

DWR. (2015a). Dayflow, an estimate of daily average delta outflow. California Department of Water Resources. Online resource available at: http://www.water.ca.gov/dayflow/. Accessed on June 20, 2015.

DWR. (2015b). Water Data Library. California Department of Water Resources. Online resource available at: http://www.water.ca.gov/waterdatalibrary/. Accesed June 21, 2015.

Elena, G.-d.-C., & Esther, V. (2010). From water to energy: The virtual water content and water footprint of biofuel consumption in Spain. Energy Policy, 38(3), 1345-1352. doi: http://dx.doi.org/10.1016/j.enpol.2009.11.015

Escriva-Bou, A., Lund, J. R., & Pulido-Velazquez, M. (2015a). Modeling residential water and related energy, carbon footprint and costs in California. Environmental Science & Policy, 50(0), 270-281. doi: http://dx.doi.org/10.1016/j.envsci.2015.03.005

Escriva-Bou, A., Lund, J. R., & Pulido-Velazquez, M. (2015b). Optimal residential water conservation strategies considering related energy in California. Water Resources Research, 51(6), 4482-4498.

Escriva-Bou, A., Pulido-Velazquez, M., & Pulido-Velazquez, D. (2017). Economic value of climate change adaptation strategies for water management in Spain's Jucar basin. *Journal of Water Resources Planning and Management*, *143*(5), 04017005.

Faunt, Claudia C., et al. "Water Availability and Land Subsidence in the Central Valley, California, USA." Hydrogeology Journal 24.3 (2016): 675-684.

Fidar, A., Memon, F. A., & Butler, D. (2010). Environmental implications of water efficient microcomponents in residential buildings. Science of the Total Environment, 408(23), 5828-5835. doi: DOI 10.1016/j.scitotenv.2010.08.006

Francés, F., Vélez, J. J., Vélez, J., & Puricelli, M. (2002). Distributed modelling of large basins for a real time flood forecasting system in Spain. Paper presented at the Second Federal Interagency Hydrologic Modeling Conference.

Gleick, P. H. (1994). Water and energy. Annual Review of Energy and the environment, 19(1), 267-299.

Giupponi, C., Mysiak, J., Fassio, A., & Cogan, V. (2004). MULINO-DSS: a computer tool for sustainable use of water resources at the catchment scale. Mathematics and Computers in Simulation, 64(1), 13-24. doi: DOI 10.1016/j.matcom.2003.07.003

Griffin, R. C. (2016). Water resource economics: the analysis of scarcity, policies, and projects. MIT Press.

Hanak, E. *et al.* Managing California's Water: From Conflict to Reconciliation. Report No. 978-1-58213-141-2, (Public Policy Institute of California, San Francisco, CA, 2011).

Harbaugh, A. W. (2005). MODFLOW-2005, the US Geological Survey modular ground-water model: The ground-water flow process: US Department of the Interior, US Geological Survey Reston, VA, USA.

Hardy, L., Garrido, A., & Juana, L. (2012). Evaluation of Spain's Water-Energy Nexus. International Journal of Water Resources Development, 28(1), 151-170. doi: Doi 10.1080/07900627.2012.642240

Harou, J. J., Medellín - Azuara, J., Zhu, T., Tanaka, S. K., Lund, J. R., Stine, S., ... & Jenkins, M. W. (2010). Economic consequences of optimized water management for a prolonged, severe drought in California. Water Resources Research, 46(5).

Healy, R. W., Alley, W. M., Engle, M. A., McMahon, P. B., & Bales, J. D. (2015). The water-energy nexus—An earth science perspective: U.S. Geological Survey Circular 1407, 107 p., http://dx.doi.org/10.3133/cir1407.

ITRC. (2015). California Evapotranspiration Data for Irrigation District Water Balances. Irrigation Training & Research Center. CalPoly. San Luis Obispo. Online resource available at: http://www.itrc.org/etdata/waterbal.htm. Accessed on June 20, 2015.

Jackson, T. M., Khan, S., & Hafeez, M. (2010). A comparative analysis of water application and energy consumption at the irrigated field level. Agricultural Water Management, 97(10), 1477-1485. doi: DOI 10.1016/j.agwat.2010.04.013

Kenway, S. J., Scheidegger, R., Larsen, T. A., Lant, P., & Bader, H. P. (2013). Water-related energy in households: A model designed to understand the current state and simulate possible measures. Energy and Buildings, 58, 378-389. doi: DOI 10.1016/j.enbuild.2012.08.035

Labadie, J. (2005). MODSIM: River basin management decision support system. Watershed Models. CRC Press, Boca Raton, Florida.

Livneh, B., Rosenberg, E. A., Lin, C. Y., Nijssen, B., Mishra, V., Andreadis, K. M., . . . Lettenmaier, D. P. (2014). A long-term hydrologically based dataset of land surface fluxes and states for the conterminous United States: Update and extensions (vol 26, pg 9384, 2013). Journal of Climate, 27(1), 477-486. doi: Doi 10.1175/Jcli-D-13-00697.1

Loucks, D. P., Van Beek, E., Stedinger, J. R., Dijkman, J. P., & Villars, M. T. (2005). *Water resources systems planning and management: an introduction to methods, models and applications*. Paris: Unesco.

Macknick, J., Newmark, R., Heath, G., & Hallett, K. C. (2012). Operational water consumption and withdrawal factors for electricity generating technologies: a review of existing literature. Environmental Research Letters, 7(4). doi: Artn 045802 Doi 10.1088/1748-9326/7/4/045802

Maupin, M. A., Kenny, J. F., Hutson, S. S., Lovelace, J. K., Barber, N. L., & Linsey, K. S. (2014). Estimated use of water in the United States in 2010: US Geological Survey.

Mielke, E., Diaz Anadon, L., & Narayanamurti, V. (2010). Water consumption of energy resource extraction, processing, and conversion. Energy Technology Innovation Policy Research Group. Harvard Kennedy School. Belfer Center for Science and International Affairs. October 2010.

Mo, W. W., Wang, R. R., & Zimmerman, J. B. (2014). Energy-Water Nexus Analysis of Enhanced Water Supply Scenarios: A Regional Comparison of Tampa Bay, Florida, and San Diego, California. Environmental Science & Technology, 48(10), 5883-5891. doi: Doi 10.1021/Es405648x

Mo, W. W., Zhang, Q., Mihelcic, J. R., & Hokanson, D. R. (2011). Embodied energy comparison of surface water and groundwater supply options. Water Res, 45(17), 5577-5586. doi: DOI 10.1016/j.watres.2011.08.016

Morales, M. A., Heaney, J. P., Friedman, K. R., & Martin, J. M. (2013). Parcel-level model of water and energy end use: Effects of indoor water conservation. Journal American Water Works Association, 105(9), 83-84.

Mount, J., C. Chappelle, B. Gray, E. Hanak and J. Lund (2016). *The Sacramento-San Joaquin Delta*. Public Policy Institute of California.

Munoz, I., Mila-i-Canals, L., & Fernandez-Alba, A. R. (2010). Life Cycle Assessment of Water Supply Plans in Mediterranean Spain. Journal of Industrial Ecology, 14(6), 902-918. doi: DOI 10.1111/j.1530-9290.2010.00271.x

Nair, S., George, B., Malano, H. M., Arora, M., & Nawarathna, B. (2014). Water-energy-greenhouse gas nexus of urban water systems: Review of concepts, state-of-art and methods. Resources Conservation and Recycling, 89, 1-10. doi: DOI 10.1016/j.resconrec.2014.05.007

Pathak, T. B., Maskey, M. L., Dahlberg, J. A., Kearns, F., Bali, K. M., & Zaccaria, D. (2018). Climate Change Trends and Impacts on California Agriculture: A Detailed Review. *Agronomy*, *8*(3), 25.

Plappally, A. K., & Lienhard, J. H. (2012). Energy requirements for water production, treatment, end use, reclamation, and disposal. Renewable & Sustainable Energy Reviews, 16(7), 4818-4848. doi: DOI 10.1016/j.rser.2012.05.022

Raluy, R. G., Serra, L., Uche, J., & Valero, A. (2004). Life-cycle assessment of desalination technologies integrated with energy production systems. Desalination, 167(1-3), 445-458. doi: DOI 10.1016/j.desal.2004.06.160

Reffold, E., Leighton, F., Choufhoury, F., & Rayner, P. (2008). Greenhouse gas emissions of water supply and demand management. Science Report No SC070010. Environment Agency; 2008.

Rodríguez-Díaz J.A, Camacho-Poyato E., Blanco-Pérez M., 2011. Evaluation of water and energy use in pressurized irrigation networks in Southern Spain. J Irrig Drain Eng. doi:10.1061/(ASCE)IR.1943-4774. 0000338.

Roy, S. B., Chen, L., Girvetz, E. H., Maurer, E. P., Mills, W. B., & Grieb, T. M. (2012). Projecting water withdrawal and supply for future decades in the US under climate change scenarios. *Environmental science & technology*, *46*(5), 2545-2556.

Sanders, K. T., & Webber, M. E. (2012). Evaluating the energy consumed for water use in the United States. Environmental Research Letters, 7(3). doi: Artn 034034 Doi 10.1088/1748-9326/7/3/034034

Scanlon, B. R., Duncan, I., & Reedy, R. C. (2013). Drought and the water-energy nexus in Texas. Environmental Research Letters, 8(4). doi: Artn 045033 Doi 10.1088/1748-9326/8/4/045033

Scanlon, B. R., Faunt, C. C., Longuevergne, L., Reedy, R. C., Alley, W. M., McGuire, V. L., & McMahon, P. B. (2012). Groundwater depletion and sustainability of irrigation in the US High Plains and Central Valley. Proceedings of the National Academy of Sciences of the United States of America, 109(24), 9320-9325. doi: DOI 10.1073/pnas.1200311109

Siddiqi, A., & Anadon, L. D. (2011). The water-energy nexus in Middle East and North Africa. Energy Policy, 39(8), 4529-4540. doi: DOI 10.1016/j.enpol.2011.04.023

Sorooshian, S., Duan, Q. Y., & Gupta, V. K. (1993). Calibration of Rainfall-Runoff Models - Application of Global Optimization to the Sacramento Soil-Moisture Accounting Model. Water Resources Research, 29(4), 1185-1194. doi: Doi 10.1029/92wr02617

Spang, E. S., & Loge, F. J. (2015). A High-Resolution Approach to Mapping Energy Flows through Water Infrastructure Systems. Journal of Industrial Ecology, n/a-n/a. doi: 10.1111/jiec.12240

Spang, E. S., Holguin, A. J., & Loge, F. J. (2018). The estimated impact of California’s urban water conservation mandate on electricity consumption and greenhouse gas emissions. *Environmental Research Letters, 13(1),* 014016.

Stokes, J. R., & Horvath, A. (2009). Energy and Air Emission Effects of Water Supply. Environmental Science & Technology, 43(8), 2680-2687. doi: Doi 10.1021/Es801802h

Tidwell, V. C., Kobos, P. H., Malczynski, L. A., Klise, G., & Castillo, C. R. (2012). Exploring the Water-Thermoelectric Power Nexus. Journal of Water Resources Planning and Management-Asce, 138(5), 491-501. doi: Doi 10.1061/(Asce)Wr.1943-5452.0000222

Tidwell, V. C., Moreland, B., & Zemlick, K. (2014). Geographic Footprint of Electricity Use for Water Services in the Western US. Environmental Science & Technology, 48(15), 8897-8904. doi: Doi 10.1021/Es5016845

USDA. (2015). Agricultural Statistics Annual. National Agricultural Statistics Service. United States Department of Agriculture. Online resource available at: http://www.nass.usda.gov/Publications/Ag_Statistics/index.asp. Accesed on June 20, 2015.

USDOE. (2006). Energy demands on water resources. Report to Congress on the Interdependency of Energy and Water. U.S. Department of Energy. December 2006.

Vörösmarty, C. J., Green, P., Salisbury, J., & Lammers, R. B. (2000). Global water resources: vulnerability from climate change and population growth. *science, 289*(5477), 284-288.

Wilkinson, R. C. (2007). Analysis of the energy intensity of water supplies for West Basin Municipal Water District. West Basin Municipal Water district Report March.

Yates, D., Purkey, D., Sieber, J., Huber-Lee, A., & Galbraith, H. (2005). WEAP21 - A demand-, priority-, and preference-driven water planning model Part 2: Aiding freshwater ecosystem service evaluation. Water International, 30(4), 501-512.

Appendix

Table A1: Proportion of each county included in each cell (left) and total area of each cell accounting for the area of each county included (right)

County	Area (Sq. miles)	Area (Sq. km)	Cell 1	Cell 2	Cell 3	Cell 4	Share in Cell 1	Share in Cell 2	Share in Cell 3	Share in Cell 4
Alameda	739.02	1914.05	B1	–	–	–	100%	–	–	–
Alpine	738.33	1912.27	ES2	–	–	–	100%	–	–	–
Amador	594.58	1539.96	ES2	D2	–	–	50%	50%	–	–
Butte	1636.46	4238.42	SV2	–	–	–	100%	–	–	–
Calaveras	1020.01	2641.82	D2	–	–	–	100%	–	–	–
Colusa	1150.73	2980.38	SV1	–	–	–	100%	–	–	–
Contra Costa	715.94	1854.28	B1	–	–	–	100%	–	–	–
Del Norte	1006.37	2606.49	NC1	–	–	–	100%	–	–	–
El Dorado	1707.88	4423.39	D2	ES2	–	–	50%	50%	–	–
Fresno	5957.99	15431.13	TL1	TL2	CC2	ES4	25%	25%	10%	40%
Glenn	1313.95	3403.12	NC2	D2	–	–	75%	25%	–	–
Humboldt	3567.99	9241.06	NC1	NC2	–	–	50%	50%	–	–
Imperial	4176.60	10817.35	DS2	SS2	–	–	80%	20%	–	–
Inyo	10180.88	26368.38	ES4	ES5	–	–	50%	50%	–	–
Kern	8131.92	21061.59	TL1	TL2	TH1	TH2	10%	10%	20%	60%
Kings	1389.42	3598.58	TL1	–	–	–	100%	–	–	–
Lake	1256.46	3254.22	NC2	–	–	–	100%	–	–	–
Lassen	4541.18	11761.61	ES1	ES2	–	–	25%	75%	–	–
Los Angeles	4057.88	10509.87	SC1	TH1	–	–	75%	25%	–	–
Madera	2137.07	5534.99	SJV2	ES3	–	–	75%	25%	–	–
Marin	520.31	1347.60	B1	–	–	–	100%	–	–	–
Mariposa	1448.82	3752.43	SJV2	ES3	–	–	75%	25%	–	–
Mendocino	3506.34	9081.39	NC2	–	–	–	100%	–	–	–
Merced	1934.97	5011.55	SJV1	SJV2	–	–	75%	25%	–	–
Modoc	3917.77	10146.99	NS3	–	–	–	100%	–	–	–
Mono	3048.98	7896.83	ES3	–	–	–	100%	–	–	–
Monterey	3280.60	8496.72	CC1	CC2	–	–	80%	20%	–	–
Napa	748.36	1938.24	B1	NC2	–	–	50%	50%	–	–
Nevada	957.77	2480.61	SV2	ES1	–	–	25%	75%	–	–
Orange	790.57	2047.57	SC2	–	–	–	100%	–	–	–
Placer	1407.01	3644.14	SV2	ES1	–	–	50%	50%	–	–
Plumas	2553.04	6612.35	ES1	–	–	–	100%	–	–	–
Riverside	7206.48	18664.71	DS1	SS1	SC2	DS2	30%	50%	10%	10%
Sacramento	964.64	2498.41	D1	D2	–	–	80%	20%	–	–
San Benito	1388.71	3596.75	CC1	–	–	–	100%	–	–	–
San Bernardino	20056.94	51947.27	ES5	DS1	SS1		50%	25%	25%	–
San Diego	4206.63	10895.13	SC2	SS2	–	–	50%	50%	–	–
San Francisco	46.87	121.39	B1	–	–	–	100%	–	–	–
San Joaquin	1391.32	3603.50	D1	–	–	–	100%	–	–	–
San Luis Obispo	3298.57	8543.26	CC2	–	–	–	100%	–	–	–
San Mateo	448.41	1161.38	B1	–	–	–	100%	–	–	–
Santa Barbara	2735.09	7083.86	CC3	–	–	–	100%	–	–	–
Santa Clara	1290.10	3341.35	B1	CC1	–	–	50%	50%	–	–
Santa Cruz	445.17	1152.99	CC1	–	–	–	100%	–	–	–
Shasta	3775.40	9778.25	SJV1	NS2	–	–	25%	75%	–	–
Sierra	953.21	2468.80	ES1	–	–	–	100%	–	–	–
Siskiyou	6277.89	16259.67	NS1	NS2	–	–	50%	50%	–	–
Solano	821.77	2128.38	D1	B1	–	–	75%	25%	–	–
Sonoma	1575.85	4081.44	NC1	B1	–	–	75%	25%	–	–
Stanislaus	1494.83	3871.59	SJV1	–	–	–	100%	–	–	–
Sutter	602.41	1560.24	SV2	D2	–	–	50%	50%	–	–
Tehama	2949.71	7639.72	SV1	SV2	–	–	75%	25%	–	–
Trinity	3179.25	8234.23	NC1	NC2	–	–	20%	80%	–	–
Tulare	4824.22	12494.68	TL2	ES4	–	–	40%	60%	–	–
Tuolumne	2220.88	5752.06	D2	ES3	–	–	20%	80%	–	–
Ventura	1843.13	4773.69	SC1	TH1	–	–	70%	30%	–	–
Yolo	1014.69	2628.04	D1	–	–	–	100%	–	–	–
Yuba	631.84	1636.46	SJV2	–	–	–	100%	–	–	–

Cell	Area (Sq. Km)
NC1	11934.94
NS1	8129.84
NS2	15463.52
NS3	10146.99
NC2	27064.97
SV1	8710.17
SV2	9370.69
ES1	15704.09
B1	10590.95
D1	9826.55
D2	8904.48
ES2	13715.15
CC1	13217.78
SJV1	10074.82
SJV2	9854.91
ES3	14820.33
CC2	11785.72
TL1	9562.53
TL2	10961.82
ES4	26853.45
CC3	7083.86
TH1	8271.89
TH2	12636.95
ES5	39157.83
SC1	11223.98
SS1	22319.17
DS1	18586.23
SC2	9361.60
SS2	7611.04
DS2	10520.35